Supporting Information

Si Nanoparticles Seeded in Carbon-Coated Sn Nanowires as an Anode for High-Energy and High-Rate Lithium-Ion Batteries

Liubin Ben (贲留斌)[abc#], Jin Zhou (金周) [abc#], Hongxiang Ji (季洪祥)[abc], Hailong Yu(俞海龙)[abc], Wenwu Zhao (赵文武)[abc] and Xuejie Huang (黄学杰)[abc] *

[a]Songshan Lake Materials Laboratory, Dongguan 523808, Guangdong Province, People's Republic of China

[b]Beijing National Laboratory for Condensed Matter Physics, Institute of Physics, Chinese Academy of Sciences, Beijing, 100190, China

[b]Center of Materials Science and Optoelectronics Engineering, University of Chinese Academy of Sciences, Beijing 100049, China

Corresponding Author

E-mail: xjhuang@iphy.ac.cn (Xuejie Huang)

The XRD structure of the nanosized Si and SnO_2 as starting materials for the preparation of the SiNPs-in-SnNWs anode are shown in Fig. S1. XRD patterns of the Si nanoparticles can be indexed to the *F*d-3m structure (Fig. S1a), and the SnO_2 can be indexed to the $P4_2/mnm$ structure (Fig. S1b).

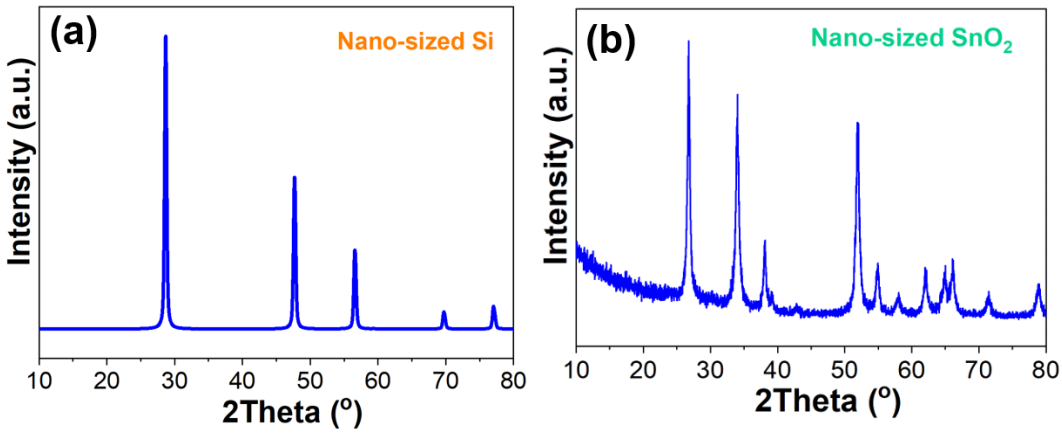

Fig. S1. XRD patterns for (a) nano-sized Si particles and (b) nano-sized SnO_2 particles.

A typical agglomerate of the SiNPs-in-SnNWs anode nanowires is illustrated in Fig $2a_1$. This was further cut by a focused ion beam (FIB), and the cut agglomerate is shown in Fig. $2a_2$. The enlarged region of the cut agglomerate clearly indicates a significant number of voids inside the agglomerate.

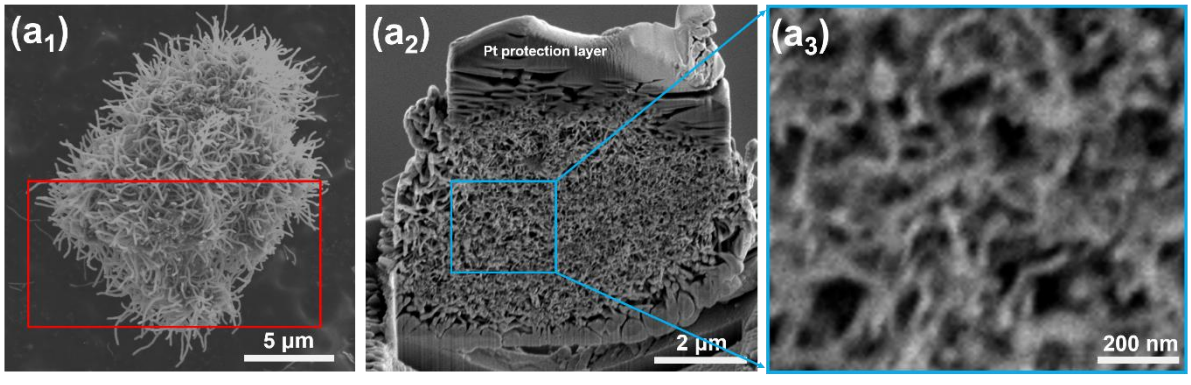

Fig. S2. FIB and SEM analysis of the SiNPs-in-SnNWs anode. (a_1) A SEM image of a typical sample for further FIB cut. (a_2, a_3) SEM images of the FIB cut agglomerate of SiNPs-in-SnNWs anode nanowires. Red rectangle in panel indicates the region for the FIB cut.

The morphology and element distribution of the anode prepared with SnNWs in a similar way to that of the SiNPs-in-SnNWs anode is shown in Fig. S3. The nanowires of the SnNWs anode are relatively straight compared to that of the SiNPs-in-SnNWs anode. EDS mapping clearly shows a homogeneous distribution of carbon and tin inside the nanowires.

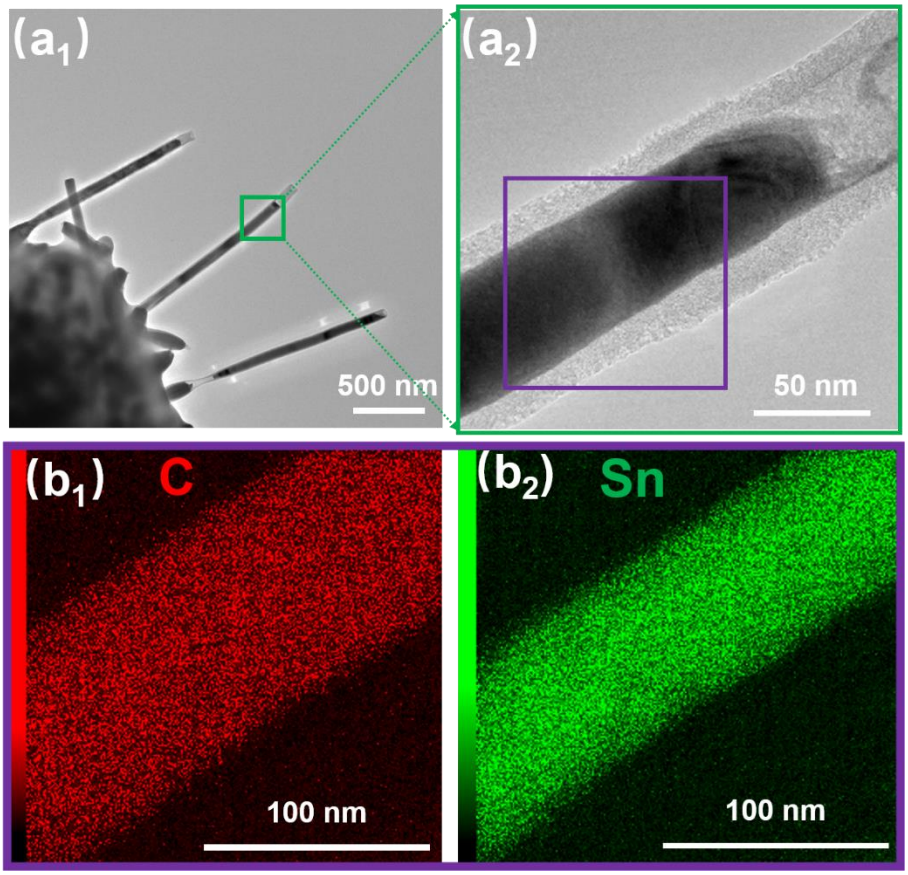

Fig. S3. (a_1,a_2) STEM-HAADF images of SnNWs anode prepared similar to SiNPs-in-SnNWs. STEM-EDS elemental mapping of (b_1) carbon and (b_2) tin elements from the region indicated by the purple square in panel a_2.

The XRD patterns of the SiNPs-in-SnNWs anode prepared after heat-treatment is shown in Gig. S4, indicating a mixture of Sn (space group $I4_1/amd$) with a small amount of Si (space group $Fd\text{-}3m$.) There was no evidence of the presence of SnO or SnO_2 in any of the analyzed anode samples.

Carbon was not detected by XRD, possibly due to its small amount or amorphous nature. The Si to Sn weight ratio in the samples, determined from the Rietveld refinement method, varied slightly, but all showed an equivalent mole ratio value close to 1 : 1.

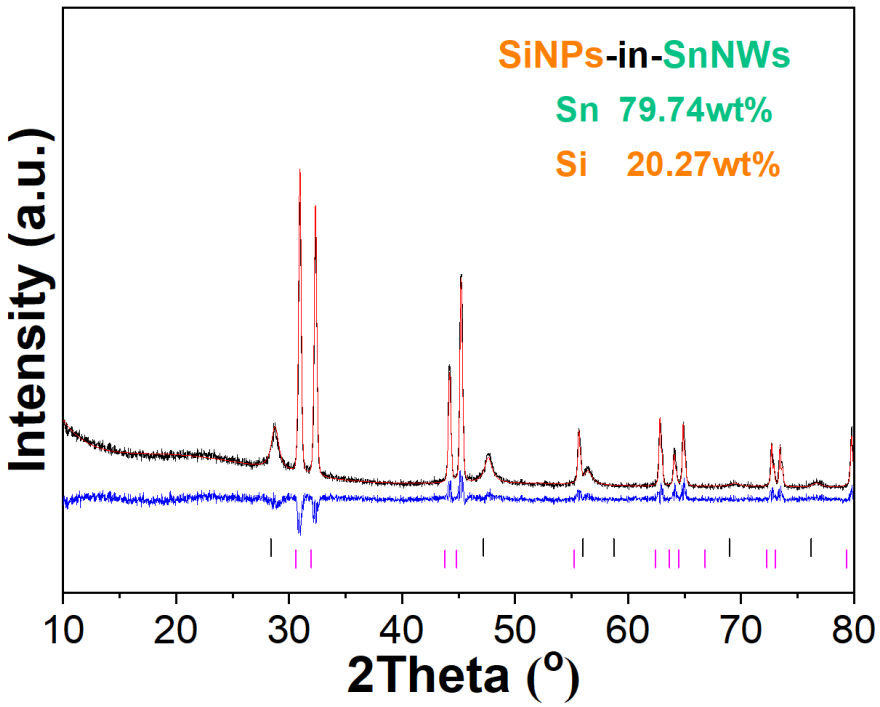

Fig. S4. Rietveld refinement of XRD patterns for the SiNPs-in-SnNWs anode after heat-treatment.

The element information of the SiNPs-in-SnNWs anode prepared after heat treatment is shown in Table S1. The content of carbon was 7.2 wt.% and the Sn : Si ratio was close to 4.22, in agreement with that of Sn : Si (4.24) in the starting material. The oxygen content was very low for all the samples, which was 0.4 wt.% after heat treatment of three hours. This suggests that SnO_2 in the starting material almost completely transforms into Sn after the heat treatment.

Table S1. The results of inductive coupled plasma (ICP) measurement for SiNPs-in-SnNWs anode prepared after heat treatment.

	C (wt%)	Sn (wt%)	Si (wt%)	O (wt%)
SiNPs-in-SnNWs	7.2	74.8	17.6	0.4

TG results, Fig. S5, showed the maximum weight change of SiNPs-in-SnNWs anode material during heating to 1200 ^{o}C was 31.6%. The following reactions occurred during the heat-treatment:

$Si + O_2 \rightarrow SiO_2$

$Sn + O_2 \rightarrow +SnO_2$

$C + O2 \rightarrow CO_2\uparrow$

Based on the reactions and mole ratio of Si and Sn, the content of C was calculated to be 7.0 wt%.

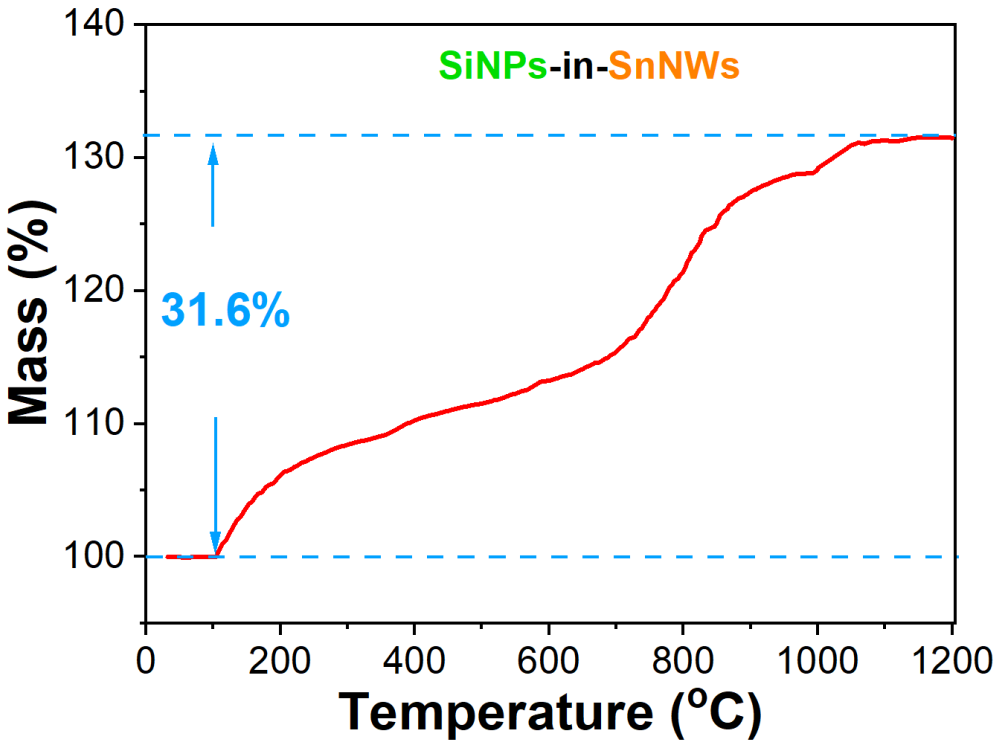

Fig. S1. TG analysis of SiNPs-in-SnNWs.

XPS analysis of the SiNPs-in-SnNWs anode shows that the Sn (Fig. S6a) on the surface of the anode and after 20-40 nm etching is still Sn^0 and the corresponding O (Fig. S6b) is very limited.

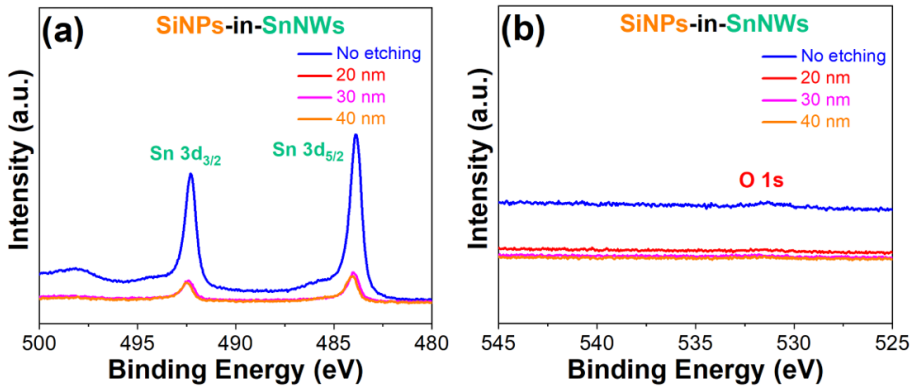

Fig. S6. XPS analysis of (a) Sn and (b) O of SiNPs-in-SnNWs anode before and after 20-40 nm etching.

A schematic arrangement of Sn atoms ($I4_1/amd$) viewed along the [1 -1 1] crystallographic direction is shown in Fig. S7a_1. The simulated electron diffraction patterns associated with Fig. S7a_1 are

shown in Fig. S7a_2, which are generally similar to the FFTs of the STEM image obtained from the surface of the nanowire, Fig. S7a_3. Note the [-1 1 0] reflections observed in panel a_2 is likely attributed to double reflections. The arrangement of Si atoms (Fd-3m) viewed along the [0 -1 1] crystallographic is shown in Fig. S7b_1. Its associated simulated electron diffraction patterns, Fig. S7b_2, are similar to the FFTs of the STEM image obtained from the center of the nanowire, Fig. S7b_3.

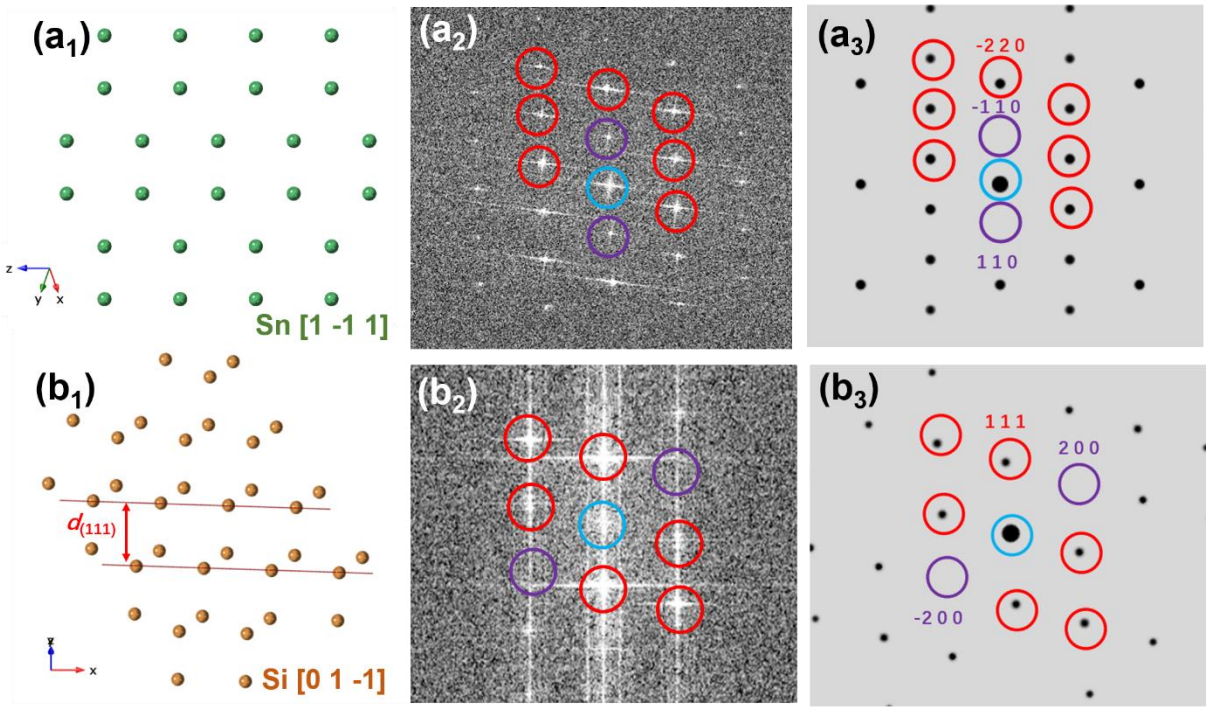

Fig. S7. (a_1) A schematic arrangement of Sn atoms viewed along the [1 -1 1] crystallographic direction of the *I*41/amd structure and (a_2) simulated electron diffraction patterns for a_1 and (a_3) FFTs of STEM image obtained from the surface of the nanowire. (b_1) a schematic arrangement of Si atoms viewed along the [0 -1 1] crystallographic direction of the *F*d-3m structure and (b_2) simulated electron diffraction patterns for b_1 and (b_3) FFTs of STEM image obtained from the center of the nanowire. Purple cycles in panel a_2-a_3, b_2-b_3 indicate systematic absent reflections.

The electrochemical impedance spectroscopy plots (EIS) for the pristine and room temperature

cycled (fiftieth cycle at 0.2 C) SiNPs, SnNWs, and SiNPs-in-SnNWs half-cells are shown in Fig. S8. Before cycling, all the half-cells exhibit a total impedance of ~50 Ω, Fig. S87a. However, after 50 cycles, the total impedance of the SiNPs half-cell increases drastically to 89.2 Ω, whereas it is only 16.5 Ω for the SnNWs and 18.3 Ω for the SiNPs-in-SnNWs half-cells, Fig. S8b. The EIS results here indicate the anode consists of Si nanoparticles seeded in Sn nanowires retains a similar electrical conductivity to that of pure Sn nanowires.

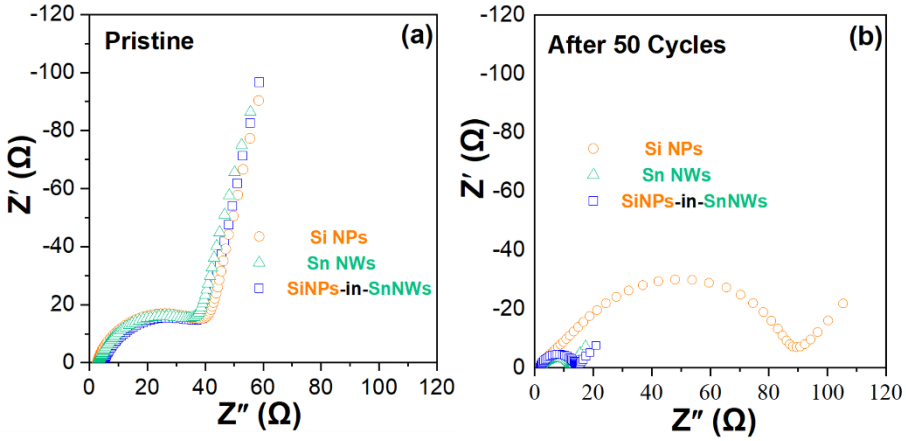

Fig. S8. Electrochemical impedance spectroscopy for the (a) pristine and (b) room temperature cycled (50 cycles at 0.2 C) SiNPs, SnNWs and SiNPs-in-SnNWs half-cells.